

# Control of spatiotemporal chaos: dependence of the minimum pinning distance on the spatial measure entropy

A. Greilich<sup>1</sup>, M. Markus<sup>1,a</sup>, and E. Goles<sup>2</sup>

<sup>1</sup> Max-Planck-Institut fuer molekulare Physiologie, Postfach 500247, 44202 Dortmund, Germany

<sup>2</sup> Centre for Mathematical Modelling, UMR 2071, CNRS-Universidad de Chile, Casilla 170-3, Santiago, Chile

Received 23 June 2004 / Received in final form 22 October 2004

Published online 3 May 2005 – © EDP Sciences, Società Italiana di Fisica, Springer-Verlag 2005

**Abstract.** We investigate the control of spatiotemporal chaos by external forcing at equidistant points (pinning sites) in one-dimensional systems. A monotonic decrease of the minimum distance between pinning sites versus the spatial measure entropy (in the absence of forcing) can be obtained for an appropriate choice of the forcing procedure. Such a relation between a feature for control and the disorder of the uncontrolled system is shown for four systems: binary cellular automata, coupled logistic equations, a stick-slip model and coupled differential equations.

**PACS.** 05.45.-a Nonlinear dynamics and nonlinear dynamical systems – 89.75.-k Complex systems

## 1 Introduction

Since about one decade, control of spatiotemporal chaos by manipulating single points (pinning sites) has been investigated [1–12]. In the present work we are concerned with the determination of the minimum distance  $d_{crit}$  between equidistant pinning sites for the control of chaotic one-dimensional systems. The systems considered here are discrete (or discretized) in time, space and phase variables. Our aim is to look for forcing procedures at the pinning sites, such that  $d_{crit}$  can be determined from a quantity that characterizes the disorder of the system. As a quantity with this property we consider in this work the spatial measure entropy [13] defined as

$$S = -\frac{1}{X} \sum_{j=1}^{k^X} p_j \log_k p_j. \quad (1)$$

$S$  is evaluated in the absence of forcing at the pinning sites. For each time step  $n = 1, 2, \dots, T$  we regard spatial cells  $i = 1, 2, \dots, L$ . Each cell can be in  $k$  states. Blocks consisting of  $X$  adjacent cells (at fixed values of  $i$  and  $n$ ) can thus be in  $k^X$  states, each one with probability  $p_j$  ( $j = 1, 2, \dots, k^X$ ). The consideration here of the spatial measure entropy is to be contrasted with previous works on coupled map lattices [10,11], in which pinning was related to the Lyapunov exponents.

In Section 2, we consider cellular automata with binary phase variables, as proposed by Wolfram [13]. In the third (coupled logistic maps), in the fourth (stick-slip model) and in Section 5 (coupled Lorenz equations)

the phase variables are discretized by dividing the interval between the minimum and the maximum of each variable into  $k$  equal intervals; the variables are set constant within each of these intervals.

We use periodical boundary conditions for the phase variables  $x_n(i)$ , i.e.  $x_n(i+L) = x_n(i)$ . Calculations are performed starting with values of  $x_1(i)$  chosen randomly and equally distributed within the sets under consideration. Both  $d_{crit}$  and  $S$  are determined out of 100 runs with different initial conditions. All evaluations are started in each run after 3000 time steps in order to allow transients to die away. Any value of  $T$  given below includes these 3000 steps. The following criterium is used for the determination of  $d_{crit}$ : for  $d < d_{crit}$ , the system becomes periodical everywhere and for all runs; for  $d \geq d_{crit}$ , the system remains chaotic in at least one cell in some run.

The rationale of this work is the following. By common sense one expects that a larger  $S$  (as a measure of disorder in the absence of control) requires denser control, i.e. smaller values of  $d_{crit}$ . Thus, one expects a monotonously decreasing dependence of  $d_{crit}$  versus  $S$ . We ask if such a dependence actually holds.

## 2 Binary cellular automata

As simplest examples for spatially extended chaotic systems, we consider binary ( $k = 2$ ) Wolfram-automata [13]. We assume that  $x_{n+1}(i)$  is a function  $\Phi$  of  $\rho$ , where  $\rho$  is the sum of the values  $x_n(m)$  for  $m = i-2, i-1, i, i+1, i+2$  (totalistic rule with neighbourhood  $r = 2$ ). The rules

<sup>a</sup> e-mail: mario.markus@mpi-dortmund.mpg.de

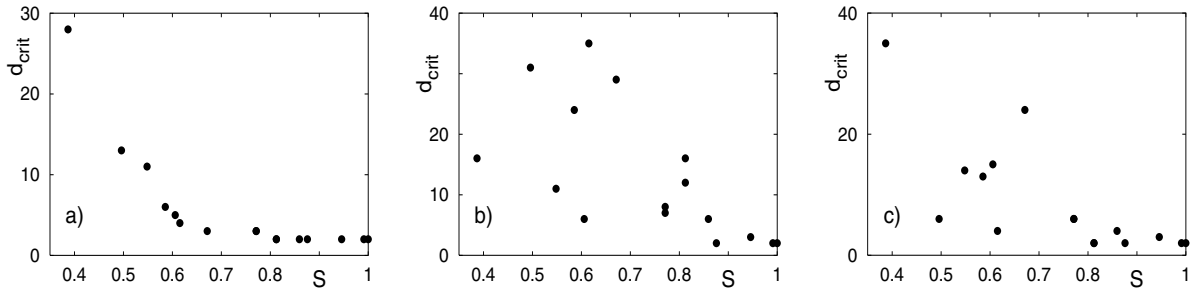


**Fig. 1.** (a) Minimum distance between pinning sites  $d_{crit}$  versus the spatial measure entropy  $S$  for all totalistic Wolfram automata leading to chaos for  $k = r = 2$ ; each point in the figure corresponds to one automaton rule; the pinning sites are forced by setting 001100... if initially 0 and 110011... otherwise.  $L = 5000$ ,  $T = 30000$ ,  $X = 5$ . (b) As (a), but setting the rule with code  $K = 24$  at the pinning sites. (c) As (a), but forcing the pinning sites with 010101... if initially 0 and 101010... otherwise.

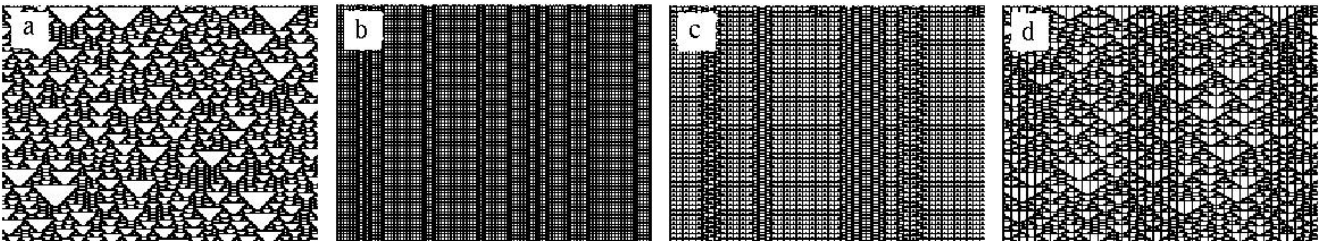


**Fig. 2.** (a) Illustration of an uncontrolled Wolfram automaton ( $r = k = 2$ , rule  $K = 28$ ). (b) Control with  $d = 2$ . (c) Control with  $d = 4$ . (d) Failure of control with  $d = d_{crit} = 5$ .

are coded by

$$K = \sum_{\rho=0}^5 2^{\rho} \Phi(\rho). \quad (2)$$

Chaotic patterns are obtained for the 16 cellular automata having codes  $K = 2, 6, 10, 12, 14, 18, 22, 26, 28, 30, 34, 38, 42, 44, 46$  and  $50$ .

We consider the following procedures for forcing at the pinning sites; (i) setting the value 0; (ii) setting the value 1; (iii) setting 000... after 0 and setting 111... after 1; (iv) setting 0101... if the first value is 0 and setting 1010... if the first value is 1; (v) setting 00110011... if the first value is 0 and setting 11001100... if the first value is 1; (vi) setting 000111000111... if the first value is 0 and 111000111000... if the first value is 1; (vii) applying rules which taken alone yield homogeneity or periodicity (for example:  $K = 4, 8, 24, 32, \dots$ ). For the cases (i) through (vi) there is no feedback of the system on the forcing; for the case (vii) there is feedback since the values assigned to each cell depend on the states in the neighbourhood, regardless of whether the cell is a pinning site or not.

Out of the forcing procedures (i) through (vii) given in the preceding paragraph, we found that one procedure, namely (v), i.e. setting 001100... or 110011..., yielded a monotonic decrease of  $d_{crit}$  vs.  $S$ . This is shown in Figure 1a. For comparison, we illustrate in Figure 1b (forcing with rule 24) and in Figure 1c (forcing with 0101... or 1010...) cases of non-monotonicity.

The meaning of  $d_{crit}$  is illustrated in Figure 2 for the rule  $K = 28$ . No control was performed in Figure 2a. Figures 2b through 2d show the outcome with increasing

values of  $d$ . Control was performed using procedure (ii). Periodicity is obtained for  $d = 2$  (Fig. 2b),  $d = 3$  and  $d = 4$  (Fig. 2c), whereas chaos remains for  $d = d_{crit} = 5$  (Fig. 2d).

By changing  $T$  and  $L$  we found that the  $d_{crit}(S)$ -dependence saturates for  $L > 4000$  and  $T > 20000$ . Figure 3a and 3b illustrate how decreasing  $L$  or  $T$  below these saturating values causes changes of the  $d_{crit}(S)$ -dependence. The choice of  $X$  does change the  $d_{crit}(S)$ -dependence but does not affect monotonicity, as illustrated in Figure 3c.

Note that by setting  $r = 2$ , information can flow across the pinning sites. Thus, control is not caused by subdivision into short automata with boundary conditions imposed at the pinning sites. This allows e.g. the CA in Figure 4d to display a similar chaotic pattern as the CA in Figure 4a.

### 3 Coupled logistic equations

Lattices of coupled maps are widely used, simple models for the study of spatiotemporal chaos [7–12, 14–19]. A prototype (see [11, 12, 14–19]) is

$$x_{n+1}(i) = F_n(i-1, i, i+1), \quad (3)$$

where

$$F_n(i-1, i, i+1) = (1 - \varepsilon) f[x_n(i)] + \frac{\varepsilon}{2} \{f[x_n(i-1)] + f[x_n(i+1)]\}. \quad (4)$$

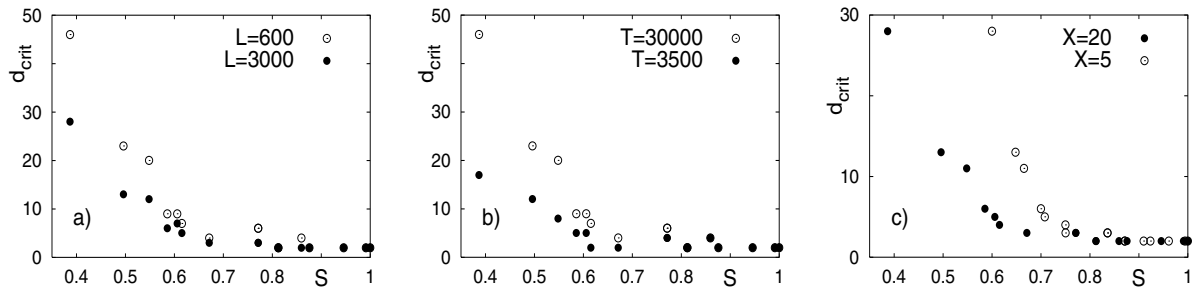


**Fig. 3.** Control of Wolfram automata. (a) As Figure 1a, but with different automaton lengths  $L$ ;  $T = 30\,000$ . (b) As Figure 1a, but with varying total times  $T$ ;  $L = 600$ . (c) As Figure 1a, but with varying block sizes  $X$ ;  $L = 5000$ ,  $T = 30\,000$ .

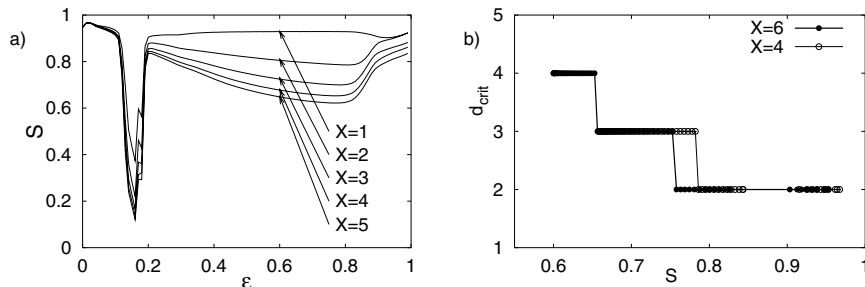


**Fig. 4.** Control of a coupled map lattice. (a)  $S$  versus the coupling parameter  $\varepsilon$  for different block sizes  $X$ . (b) Minimum distance  $d_{crit}$  between pinning sites versus  $S$  for different  $X$ .

As map  $f$  we use the chaotic logistic equation  $f(x) = 4x(1-x)$ .  $\varepsilon$  is a parameter describing the coupling between neighbouring cells. We set pinning sites as in [8]:

$$x_{n+1}(i) = F_n(i-1, i, i+1) + \sum_{j=0}^{L/d} \delta(i-dj-1)g_n, \quad (5)$$

where  $\delta(m) = 1$  if  $m = 0$  and  $\delta(m) = 0$  otherwise.  $g_n$  is given by

$$g_n = (1-\varepsilon)q(i) + \frac{\varepsilon}{2}q(i-1) + \frac{\varepsilon}{2}q(i+1). \quad (6)$$

Here,  $q(m) = px_n(m)[x_n(m) - \xi]$ .  $p$  is the feedback strength and  $\xi$  is a reference state, which is set to the unstable fixed point of the logistic equation, i.e.  $\xi = 3/4$ .

Spatial measure entropies are determined by discretizing the  $x_n(i)$  into  $k$  states, as described in the introduction. We found that  $S$  varied less than 6% when varying  $k$  between 2 and 20; this weak dependence of  $S$  on  $k$  facilitates our choice of  $k$ ; we set  $k = 10$ . The dynamics and thus the entropy was varied by changing the coupling parameter  $\varepsilon$ . We set  $p = 2.65$ . The  $\varepsilon$ -values in the systems in which we carried out control are those of the abscissa of Figure 4a, excluding the interval (0.1, 0.2), within which the behaviour without control is periodical, as indicated by the downwards peak of  $S$ .

Figure 4b shows a monotonic decrease of  $d_{crit}$  versus  $S$ . The choice of  $X$  here does not alter the monotonicity. In fact,  $X$  only shifts the  $d_{crit}(S)$ -curves horizontally as a result of the vertical shifts (on varying  $X$ ) in Figure 4a. Note that the gap around  $S = 0.87$  in Figure 4b corresponds to the downwards peaks in Figure 4a (non-chaotic behaviour in the absence of control).

The  $d_{crit}(S)$ -curves retain their monotonicity, but are shifted by changing  $T$  or  $L$ . We have set here  $T = 30\,000$  and  $L = 600$ , which are values for which saturation of  $d_{crit}(S)$  with respect to  $T$  and  $L$  occurs.

## 4 A stick-slip model

A simplified description of earthquakes is obtained with a stick-slip model (see [20]), which is constructed here as follows. A one-dimensional array of blocks connected by springs (continental plate) is placed over the rigid oceanic plate. The variable  $x_n(i)$  is the potential energy of block  $i$  at time  $n$ . A block slips if  $x_n(i) \geq 2$ ,  $x_n(i)$  becoming zero after slipping and delivering the energy  $(x_n(i) - \sigma)/2$  to each neighbour;  $\sigma$  is the energy dissipation. An earthquake occurs if at least one block slips. After the start of an earthquake all blocks come to rest due to dissipation; this relaxation may last several time steps, corresponding to seconds or minutes in nature. It is assumed that after relaxation, i.e. after an earthquake has finished, the relative movement of the plates causes an increase of the energy of each block by a constant value, which we set equal to 1. This increase in energy takes place during one time step in the simulations, but lasts years or more in nature. Thereafter, slipping and relaxation occur again. The process is described by the following map:

$$x_{n+1}(i) = x_n^+(i) + x_n^-(i) + x_n^o(i). \quad (7)$$

$x_n^+(i)$  and  $x_n^-(i)$  are the contributions from the block at the right and left, respectively;  $x_n^o(i)$  is the contribution

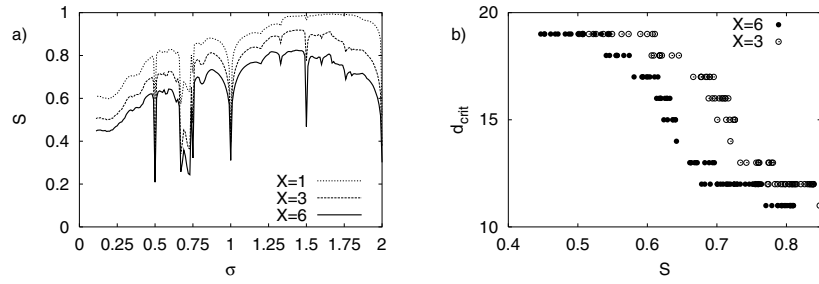


**Fig. 5.** Control of stick-slip processes. (a) Entropy  $S$  vs. dissipation parameter  $\sigma$ ; (b)  $d_{crit}$  vs.  $S$ .

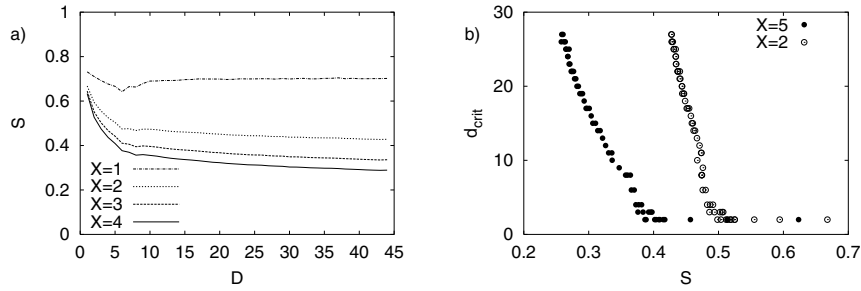


**Fig. 6.** Control of coupled differential equations. (a) Entropy  $S$  vs. diffusion coefficient  $D$ ; (b)  $d_{crit}$  vs.  $S$ .

of the considered block itself

$$x_n^\pm(i) = \begin{cases} [x_n(i \pm 1) - \sigma]/2, & x_n(i \pm 1) \geq 2 \\ 0, & \text{else} \end{cases} \quad (8)$$

$$x_n^0(i) = \begin{cases} x_n(i), & x_n(i) < 2 \\ 0, & \text{else} \end{cases}. \quad (9)$$

For the calculation of  $S$  with equation (1) we discretise the potential energy as described in Section 1, setting  $k = 10$ . As initial conditions we set randomly chosen, equally distributed values  $0 \leq x_1(i) < 2$ . As in the case of the coupled logistic equations in Section 3, we found that  $S$  is only slightly affected by the choice of  $k$  around our chosen value  $k = 10$ . Figure 5a shows  $S$  versus the dissipation  $\sigma$  for different  $X$ . The downwards peaks in this figure indicate periodical islands; the intervals of  $\sigma$  corresponding to these peaks are, of course, not subjected to control.

Control is performed by setting — at the pinning sites — the average of  $x_n(i)$  over all  $i$ ; this is done at each time step during earthquakes. The idea behind this averaging is to drive the system into a state that is closer to homogeneity. Using this procedure, we obtain nearly monotonously decreasing  $d_{crit}(S)$ -relations, as shown in Figure 5b. Note that  $X$  only shifts the  $d_{crit}(S)$ -curves horizontally, correspondingly to the vertical shifts in Figure 5a, preserving the nearly monotonic behaviour. We set  $L = 600$  and  $T = 45\,000$ , for which saturation of  $d_{crit}$  with respect to  $L$  and  $T$  occurs.

## 5 Coupled differential equations

We consider diffusively coupled Lorenz equations, as in [6]. In a spatially discrete system, we write for each cell  $i$  the Lorenz equations with a coupling term  $C$ :

$$\begin{aligned} dx(i)/dt &= \sigma(y(i) - x(i)) + C(i) \\ dy(i)/dt &= rx(i) - x(i)z(i) - y(i) + C(i) \\ dz(i)/dt &= -bz(i) + x(i)y(i) + C(i) \end{aligned} \quad (10)$$

where we assumed, as in [6], that coupling occurs only via the  $y(i)$ . We set

$$C(i) = D[0.5y(i-2) + y(i-1) - 3y(i) + y(i+1) + 0.5y(i+2)], \quad (11)$$

which is a particular mask for the discretization of the Laplace operator [21].  $D$  is the diffusion coefficient. In addition, time is discretized by replacing the left-hand sides of equations (10) by the difference quotients  $[\zeta_{n+1}(i) - \zeta_n(i)]/\Delta t$ ,  $\zeta = x, y, z$ . In this way we obtain coupled three-dimensional time-discrete maps. Setting  $\sigma = 10$ ,  $r = 28$ ,  $b = 8/3$  and  $\Delta t = 0.01$ , spatiotemporal chaos is obtained.

We determine  $S$  by considering the  $y(i)$  only. We set  $k = 10$ ; as in the cases in the previous sections, the results were not significantly affected by this choice. Figure 6a shows how  $S$  is changed by changing  $D$ . Control is performed by replacing  $r = 28$  into  $r = 0.5$  at the pinning sites. Note that if  $r = 0.5$  was set everywhere, the fixed point attractor  $(0, 0, 0)$  would be reached by each cell.  $d_{crit}$  versus  $S$  (Fig. 6b) is nearly monotonously decreasing.

We set  $L = 600$  and  $T = 30\,000$ , for which saturation of  $d_{crit}$  with respect to  $L$  and  $T$  occurs. The choice of  $X$  shifts  $d_{crit}(S)$  horizontally, as expected from the vertical shifts in Figure 6a. Note in Figure 6b that in a few cases values of  $d_{crit}$  differing by 1 are obtained for the same  $S$ ; this is a result of varying sets of initial conditions.

## 6 Conclusions

In previous works the minimum distance  $d_{crit}$  of pinning sites was determined either by numerical optimization separately for each set of control parameters, or analytically with a linear approximation around the reference state  $\xi$  for coupled map lattices. In the analyses of these lattices [10,11], control was related to the Lyapunov exponents of the system.

In the present work, we presented an alternative approach by relating the spatial measure entropy  $S$  (in the absence of control) to the minimum pinning distance  $d_{crit}$  for control. We showed a monotonic decrease of  $d_{crit}$  versus  $S$  for four different systems: Wolfram's automata, coupled logistic equations, a tectonic model and coupled Lorenz equations. This monotonic dependence saturates for sufficiently large times  $T$  and lengths  $L$ . We are as yet unable to explain the existence of forcing procedures at the pinning sites for which no monotonicity is obtained, as we found in several cases for Wolfram's automata (see e.g. Figs. 1b and 1c). Therefore, an open future task is to find necessary conditions that the forcing must fulfill for monotonicity to hold.

In cases in which one obtains fluctuations of  $d_{crit}(S)$  (Fig. 5b around  $S = 0.55$ ,  $S = 0.61$  and  $S = 0.69$ , as well as Fig. 6b around  $S = 0.4$ ), one should obviously perform control with the minimum  $d_{crit}$  within the fluctuation range.

We must remark that because of limitations in computing time, we did not obtain saturation of  $S$  with respect to  $X$ . However, this did not turn out to be a drawback, since we found that monotonicity is independent of the choice of  $X$  for all investigated models.

While it is reasonable to determine control conditions by analyzing the perturbed system, as e.g. in [10,11]), we found here a relationship of  $d_{crit}$  with a property of the unperturbed system, namely  $S$ . This is an empirical result that calls for further investigation.

Another future task concerns the spatial distribution of pinning sites. We have set here (as e.g. in [8]) equidistant pinning sites. In contrast, it is promising to consider the results of Grigoriev et al. [10] for coupled map lattices: an appropriate choice of non-equidistant sites allows control with a substantially lower pinning density.

A.G. and M.M. thank the Centre for Mathematical Modelling (Santiago, Chile) for hospitality and financial support.

## References

1. G. Hu, K.F. He, Phys. Rev. Lett. **71**, 3794 (1993)
2. J.H. Gao, J.H. Xiao, Y.G. Yao, G. Hu, Comm. theor. Phys. **32**, 481 (1999)
3. C.G. He, Z.T. Cao, Acta Phys. Sinica **50**, 2103 (2001)
4. S. Mizokami, Y. Ohishi, H. Ohashi, Physica A **239**, 227 (1997)
5. J.E. Moreira, F.W.S. Lima, J.S. Andrade, Phys. Rev. E **52**, R2129 (1995)
6. S. Jankowski, A. Londei, A. Lozowski, C. Mazur, Int. J. Circuit Theor. Appl. **24**, 275 (1996)
7. N. Parekh, S. Sinha, Physica A **318**, 200 (2003)
8. G. Hu, Z. Qu, Phys. Rev. Lett. **72**, 68 (1994)
9. Y. Ohishi, H. Ohashi, M. Akiyama, Jpn J. Appl. Phys. **34**, L1420 (1995)
10. R.O. Grigoriev, M.C. Cross, H.G. Schuster, Phys. Rev. Lett. **79**, 2795 (1997)
11. Y.S. Kwon, S.W. Ham, K.K. Lee, Phys. Rev. E **55**, 2009 (1997)
12. N. Parekh, S. Parthasarathy, S. Sinha, Phys. Rev. Lett. **81**, 1401 (1998)
13. S. Wolfram, Physica D **10**, 1 (1984)
14. X. Zhang, K. Shen, Phys. Rev. E **63**, 046212 (2001)
15. K. Kaneko, Progr. Theor. Phys. **74**, 1033 (1985)
16. J.P. Crutchfield, K. Kaneko, Phys. Rev. Lett. **60**, 2715 (1988)
17. J.D. Keeler, J.D. Farmer, Physica D **23**, 413 (1986)
18. E.J. Ding, Y.N. Lu, J. Phys. A **25**, 2897 (1992)
19. P. Parmananda, M. Hildebrand, M. Eiswirth, Phys. Rev. E **56**, 239 (1997)
20. P. Bak, C. Tang, J. Geophys. Res. **94**, 15635 (1989)
21. J.R. Weimar, J.J. Tyson, L.T. Watson, Physica D **55**, 309 (1992)